Journal of Inflammation Research

Dovepress
Taylor & Francis Group

Open Access Full Text Article

ORIGINAL RESEARCH

Wenqing Yin Attenuates the Allergic Contact Dermatitis Response by Inhibiting the JAK2/STAT1 and MAPK Signaling Pathways

Mengyue Ren[1,*], Siman Li[1,*], Shaoqiang Li[2], Zhiwei Tan[1], Jun Shi[1]

[1]School of Chinese Materia Medica, Guangdong Pharmaceutical University, Guangzhou, Guangdong, 510000, People's Republic of China; [2]Guangdong Second Traditional Chinese Medicine Hospital (Guangdong Research Institute of Traditional Chinese Medicine Manufacturing Technology), Guangzhou, Guangdong, 510000, People's Republic of China

*These authors contributed equally to this work

Correspondence: Mengyue Ren; Jun Shi, School of Chinese Materia Medica, Guangdong Pharmaceutical University, Guangzhou, Guangdong, 510000, People's Republic of China, Email Rmy0711@163.com; shijun8008@163.com

Objective: Allergic contact dermatitis (ACD) is a delayed-type inflammatory skin illness, and its incidence rate is 10–20%. Wenqing Yin (WQY) is a classic prescription commonly used to treat ACD in China and Japan, and this study aims to explore the pharmacological effect and therapeutic mechanism of WQY to treat ACD.

Methods: The pharmacological effect of WQY were investigated using a mouse model caused by 2,4-dinitrofluorobenzene, and the Th1 and Th2 cells numbers in spleen were measured. The potential active components and signal pathways of WQY to treat ACD were obtained using UPLC-MS/MS and network pharmacological analysis, the protein expression levels in relation to the MAPK and JAK/STAT1 signaling pathways were assessed, and the serum metabolites were also analyzed.

Results: WQY alleviated pathological injuries and reduced the increase in mast cells, reduced the thickness and weight of the ears, down-regulated the IL-6, IL-1β, IFN-γ, IL-4, T-bet, and STAT1 mRNA levels, and decreased the percentages of Th1 cells in spleen mononuclear cells of ACD mice. Meanwhile, 38 ingredients in WQY-containing serum were identified by UPLC–MS/MS, and 123 overlapping target genes of WQY and ACD were then obtained. The analysis of GO and KEGG pathway enrichment of the 34 core target genes out of 123 revealed that WQY may effectively treat ACD by targeting specific biological processes, such as the MAPK and JAK-STAT signaling pathway. WQY decreased the *p*-JAK2, *p*-STAT1, *p*-ERK, *p*-JNK, and *p*-p38 expressions in the ears of ACD mice, which led to the inhibition of JAK2/STAT1 and MAPK signaling pathways in treatment of ACD.

Conclusion: WQY exhibited a significant anti-inflammatory role on DNFB-induced ACD mice via inhibiting the Th1 immune response and IL-4 secretion, which may be closely linked to the JAK2/STAT1 and MAPK signaling pathways inhibition.

Keywords: allergic contact dermatitis, Wenqing Yin, network pharmacology, 2,4-dinitrofluorobenzene, JAK2/STAT1 pathway, MAPK pathway

Introduction

Skin contact with haptens can induce allergic contact dermatitis (ACD), a delayed-type inflammatory response mostly driven by antigen-specific T helper 1 (Th1) and Th2 cells.[1] The incidence rate of ACD is as high as 15–20%, and it is characterized by cutaneous swelling and redness, as well as the presence of papules and cutaneous pruritus, and the treatment costs reach up to $400 million annually in the United States.[2] Currently, corticosteroids and immunosuppressants, such as tacrolimus, are the commonly Western medicine used to treat ACD, and despite their noticeable benefits, these medications can also cause skin atrophy, osteoporosis, type II diabetes, ischemia injury, renal toxicity, and other serious side effects.[3–5] Thus, the search for safe and effective therapy medications is crucial in ACD research.

The use of Traditional Chinese medicine (TCM) formulae to treat ACD in clinical application provides important therapeutic results with no notable adverse effects.[6,7] Wenqing Yin (WQY) is a classic prescription from the ancient

Received: 17 December 2024
Accepted: 30 April 2025
Published: 30 May 2025

Graphical Abstract

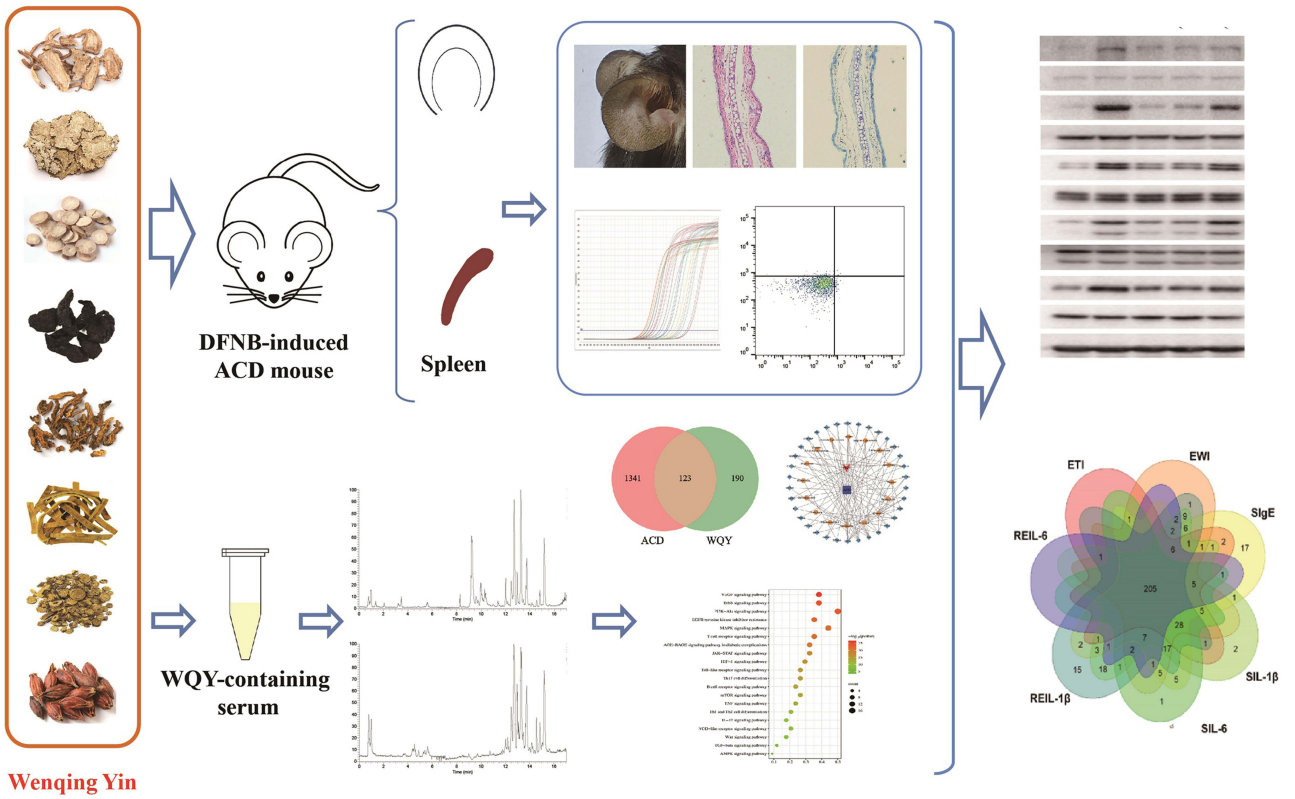

medical book of Ming Dynasty called Wanbing Huichun, and it is commonly used to treat ACD, chronic eczema, canker sore, and recurrent aphthous ulcer in China and Japan.[8–11] WQY consists of eight Chinese traditional herbs, including *Danggui* (dried roots of *Angelica sinensis* (Oliv). Diels), *Chuanxiong* (dried rhizomes of *Ligusticum sikiangense* M. Hiroe), *Baishao* (dried roots of *Cynanchum otophyllum* C.K.Schneid)., *Shudihuang* (processed rhizomes of *Rehmannia* Libosch. ex Fisch. and C.A.Mey)., *Huanglian* (dried rhizomes of *Coptis chinensis* Franch)., *Huangbo* (dried barks of *Phellodendron chinense* C.K.Schneid)., *Huangqin* (dried roots of *Scutellaria baicalensis* Georgi), and Zhizi (dried ripe fruits of *Gardenia jasminoides* J.Ellis). Out of these herbs, four of them – *Danggui, Chuanxiong, Baishao*, and *Shudihuang* – possess the capacity to nourish blood and enhance blood circulation, leading to a "warming" effect. On the other hand, the remaining four herbs – *Huanglian, Huangbo, Huangqin*, and *Zhizi* – can effectively clear heat and detoxify, working together to achieve a "clearing" effect. The combination of simultaneous warming and heat clearing in TCM is one of traditional treatment methods frequently used by Zhang Zhongjing in his book named Treatise on Febrile Diseases. Therefore, the characteristics of the combined TCM formulations from a holistic standpoint are fully reflected in the treatment of ACD using WQY.

Contemporary pharmacological investigations have revealed that WQY can considerably decrease ear swelling in ACD mice, inhibit the HaCaT cells proliferation, and increase the silk polymerization protein mRNA expression.[12,13] The current research on WQY's therapeutic potential for ACD remains limited in both scope and depth, and the existing studies are characterized by incomplete experimental designs and insufficient mechanistic investigation, particularly regarding the underlying immunomodulatory pathways. Recent studies have demonstrated that the TCM formula *Wumeiwan*, which exhibits dual warming and clearing properties similar to WQY, effectively ameliorates atopic dermatitis symptoms in murine models, and the therapeutic mechanism appears to involve attenuation of mast cell infiltration, suppression of Th2-associated cytokines, and reduction of IgE levels.[14] Therefore, the potential functional

ingredients and the underlying therapeutic mechanism of WQY were explored in this study. We explored the Th1 and Th2 immune response, detected the infiltration of mast cells and the secretion of multiple inflammatory factors, and analyzed the components of a drug-containing serum using ultrahigh-performance liquid chromatography–tandem mass spectrometry (UPLC–MS/MS) technology and constructed an ingredient-target network using network pharmacology. After that, the key targets of WQY to treat ACD were analyzed on a protein-protein interaction (PPI) network. To confirm the therapeutic mechanism of WQY to treat ACD, the proteins connected to probable signaling pathways were identified, and the serum metabolites in mice of ACD were also analyzed.

Materials and Methods

Chemicals and Reagents

Shanghai Macklin Biochemical Co., Ltd. (Shanghai, China) provided 2,4-dinitrofluorobenzene (DNFB) (lot: F830061) and olive oil (lot: C11631395). Dexamethasone (lot: D1756) and TRIzol reagent were provided by Sigma–Aldrich (St. Louis, MO, USA) and Invitrogen (Carlsbad, CA, USA). The ELISA kits for mouse interleukin 1β (IL-1β), immunoglobulin E (IgE), and IL-6 are available from CUSABIO (Wuhan, China). Gibco (Grand Island, NY, USA) provided Fetal bovine serum (FBS) and Roswell Park Memorial Institute (RPMI) 1640. Solarbio (Beijing, China) provided the red blood cell lysis buffer and TaKaRa (Osaka, Japan) provided the TB Green Premix Ex Taq II kit and Prime Script RT reagent kit. We purchased the purified rat anti-mouse CD16/CD32 antibody, anti-mouse CD3 antibody labeled with BV421, and the leukocyte activation cocktail from BD (Franklin Lakes, NJ, USA). Allophycocyanin (APC)-labeled anti-mouse interleukin (IL)-4, phycoerythrin (PE)-labeled anti-mouse interferon (IFN)-γ, and fluorescein isothiocyanate (FITC)-labeled anti-mouse CD4 antibodies, as well as intracellular fixation and permeabilization buffer set kits, were obtained from eBioscience (San Diego, CA, USA). Cell Signaling Technology, Inc. (Danvers, MA, USA) supplied rabbit monoclonal antibodies against Phospho (*p*)-Janus kinase (JAK) 2, JAK2, *p*-signal transducer and activator of transcription (STAT) 1, STAT1, *p*-p38, p38, *p*-c-Jun N-terminal kinase (JNK), JNK, *p*-extracellular signal-regulated kinase (ERK), ERK and glyceraldehyde-3-phosphate dehydrogenase (GAPDH).

Huanglian (lot: 200603441), *Huangqin* (lot: 200700791), *Huangbo* (lot: 191205031), *Zhizi* (lot: 200602991), and *Chuanxiong* (lot: 200600171) were obtained from Kangmei Pharmaceutical Co., Ltd. (Shenzhen, China). Foshan Shunde District Tiantai Pharmaceutical Co., Ltd. (Foshan, China) provided *Danggui* (lot: 200701), *Baishao* (Lot: 200901), and *Shudihuang* (lot: 200801).

Preparation of the WQY Sample

The identities of *huanglian*, *huangqin*, *huangbo*, *zhizi*, *chuanxiong*, *danggui*, *baishao*, and *shudihuang* were confirmed by Dr. Jizhu Liu, Guangdong Pharmaceutical University, P. R. China. These Chinese medicinal herbs, each weighing 15 g, were boiled for 60 min after been immersed in 1440 mL of water for 30 min. After passing through a four-layer gauze filter, the mixture was diluted to a final volume of 1200 mL with distilled water, resulting in the WQY water decoction. To obtain a high-concentration WQY (WQY-H) sample, we concentrated the WQY decoction to 1.2 $g \cdot mL^{-1}$ under reduced pressure conditions, and obtained the low-concentration WQY (WQY-L) sample by diluting the WQY-H sample twice.

HPLC Analysis of the Main Components in WQY

The major compounds of WQY were identified and quantified by HPLC on an LC-20AS HPLC (Shimadzu, Kyoto, Japan).[15] To obtain the WQY test sample, we diluted 2 mL WQY water decoction to 10 mL with methanol. Following that, we subjected the dilution to ultrasonication for 15 minutes and filtered it using a 0.45 μm microporous membrane filter after 12 h. A Polaris C18-A column (250 mm × 4.6 mm, 5 μm) (Agilent, CA, USA) was utilized for the analysis, and the mobile phase A was 0.2% phosphoric acid and B was acetonitrile. The flow rate was 0.8 mL/min, the column temperature was 30°C, the detection wavelength was 270 nm, and the gradient program used in the following way: 5%–20% B, 0–10 min; 20% B, 10–30 min; 20–24% B, 30–35 min; 24% B, 35–42 min; 24–36% B, 42–50 min; 36–38% B, 50–55 min; 38% B, 55–60 min; 38%–72% B, 60–62 min; 72–80% B, 62–70 min.

Experimental Animals

The experiment received approval from the Undergraduate Laboratory Animal Center of Guangdong Pharmaceutical University (Approval number gdpulac2020028), the Experimental Animal Center of Guangzhou University of Chinese Medicine provided the female C57BL/6J mice (20 ± 2 g) (Certificate number SCXK 2018–0034), and the welfare of the laboratory animals complied with the provisions of the Administrative Ordinance on Laboratory Animals issued by the National Commission of Science and Technology. The mice had free access to regular food and deionized water in specific-pathogen-free environments (20°C–24°C temperature and 50–60% relative humidity) for one week leading up to the experiment.

ACD Mouse Model Preparation and Drug Intervention

With a few modest modifications, the ACD mouse model was developed using data from an earlier study.[16] The abdomen of the mice was cut off within a 4 cm^2 area under isoflurane anesthesia before preparing ACD models. On day 1, the mice's shaved abdomens were sensitized topically using 30 μL of 0.5% DNFB solution, which was prepared using a blank solvent consisting of acetone and olive oil (4:1). On their right ear (both sides), the sensitized mice were exposed to 20 μL of 0.2% DNFB to generate an ACD response during days 5 and 6. The mice were divided into control, model, positive, WQY-L, and WQY-H groups in a random manner (n = 10). The mice in the model, positive, WQY-L, and WQY-H groups were modeled using DNFB as described above, and a blank solvent was utilized for sensitization and challenge of the mice in the control group. On days 1–6, the mice in the positive, WQY-L, and WQY-H groups were orally administered 2.5 $mg{\cdot}kg^{-1}$ dexamethasone, 0.6 and 1.2 $g{\cdot}mL^{-1}$ WQY (0.2 mL per 20 g body weight) once daily, respectively.

Ear Thickness and Weight Determination

To evaluate the degree of ear swelling of mice, we measured and calculated the increases in ear weight and thickness. In summary, we used a dial thickness gauge (Mitutoyo, Kanagawa, Japan) to measure the thicknesses of the right ears before sensitization and at 24 h after the last challenge, and the formula for calculating is as follows: the increase in ear thickness = thickness of challenged right ear − thickness of right ear before sensitization. A sterilized dermal biopsy punch (KAI Medical, Japan) was employed to extract round tissues measuring 4 mm in diameter in similar positions from the left and right ears of mice at 24 hours after the last challenge. The round tissues were then weighed, and the corresponding formula was used to calculate the increase in ear weight: the increase in ear weight = weight of challenged right ear − weight of unchallenged left ear. The serum of mice was obtained to detect the inflammatory cytokine and analyze the metabolites, and the spleen samples from the killed mice were aseptically extracted and kept in cold saline to isolate spleen mononuclear cells (SMC). Samples from the right ear were excised and collected for other pharmacological analyses.

Histological Analysis

The Mouse ear samples were subjected to fixation in 4% paraformaldehyde, followed by dehydration and subsequent embedding. The embedded paraffin samples were sliced into 4 μm-thick pieces and then subjected to staining with toluidine blue (TB) as well as hematoxylin and eosin (HE). To analyze and document the histopathological changes, the Olympus semi-electric fluorescence microscope (Olympus, TKY, Japan) was utilized.

Inflammatory Cytokine Analysis in Serum

The levels of IgE, IL-6, and IL-1β in the serum of mice were tested in accordance with the guidelines of the mouse IL-1β (lot: CSB-E08054m), IgE (lot: CSB-E07983m), and IL-6 (lot: CSB-E04639m-IS) ELISA kits. After adding the stop solution to the reaction, a Multiskan Sky microplate spectrophotometer (ThermoFisher, USA) was utilized to detect the absorbance at 450 nm.

Spleen Mononuclear Cells (SMCs) Isolation

With filtering through a 200-mesh filter under sterile conditions, the cells of the spleen were evenly distributed in 2 mL of phosphate-buffered saline (PBS). The cells were filled with 6 mL red blood cell lysis buffer, then inverted and placed on

ice for 15 minutes, followed by centrifugation. After being twice lysed, the cells were washed twice in PBS and once in RPMI 1640 medium before being resuspended in RPMI 1640 media supplemented with 10% FBS and eventually adjusted to a final concentration of 4×10^6/mL.

Flow Cytometry Analysis

The harvested SMCs were exposed to a leukocyte activation cocktail in a 24-well plate in CO_2 incubator (37°C) for 5 h. Subsequently, the SMCs that were washed with PBS were treated with anti-mouse CD16/CD32 antibody for 15 min at ordinary temperature to prevent nonspecific antibody binding. Anti-mouse CD3 and CD4 antibodies tagged with FITC and BV421 were used to stain the cells away from light for 30 min for surface labeling. Subsequently, an intracellular fixation and permeabilization solution was used to fix and permeate the cells. Then, the cells were treated with PE-and APC-labeled anti-mouse IFN-γ and IL-4 antibodies for 15 min, ensuring no exposure to light. After the cells were washed, a FACS Celesta flow cytometer (BD, NJ, USA) was used to identify the numbers of Th1 and Th2 cells in SMCs.

QRT-PCR Analyses

TRIzol was utilized to extract the total RNA of ear tissue samples from each group. After the genomic DNA was excised, the Prime Script RT reagent Kit was utilized to generate complementary DNA (cDNA) through a reverse transcription procedure. After preparing the PCR mix on ice, 40 cycles of qRT-PCR were run using a CFX96 Touch Real-Time PCR detection system (Bio-Rad, CA, USA). IL-1β, IL-6, IFN-γ, IL-4, T-bet, GATA binding protein (GATA)-3, STAT-1, STAT-6, and GAPDH sequences were created following our earlier research.[17] With using the $2^{-\Delta\Delta Ct}$ method, the target gene levels were normalized to GAPDH, as previously described.[18]

Analysis of the Ingredients of a Drug-Containing Serum Using UPLC–MS/MS

Ten groups (n = 3) of healthy female C57BL/6J mice (18–22 g) were orally administered 1.2 $g\cdot mL^{-1}$ WQY. Blood samples were taken at various intervals (0, 0.083, 0.25, 0.5, 1, 2, 4, 8, 12, and 24 h) after gavage, and centrifugation was used to extract the serum. The blank (0 h) and mixed drug-containing serums were mixed with four times the volume of methanol. The mixture was subjected to vortexing and subsequent centrifugation for 15 min at 12000 rpm. After that, the supernatant was dried while nitrogen gas was flowing through it. The desiccated sample was dissolved in a solution of 50% acetonitrile water, mixed vortexed, centrifugated, and the gathered supernatant was then underwent UPLC–MS/MS analysis.

The components of WQY-containing serum were identified using a Vanquish Flex ultra-HPLC coupled to an Orbitrap Exploris 120 mass spectrometer system (Thermo Fisher Scientific, MA, USA). The column temperature was 35 °C, the mobile phase A was acetonitrile (containing 0.1% formic acid), B was 0.1% formic acid, the flow was 0.3 mL/min, and the gradient program used in the following way: 5–25% A, 0–5 min; 25–60% A, 5–10 min; 60–80% A, 10–15 min; 80–90% A, 15–17 min. Both negative and positive ion electrospray ionization (ESI) were used, with the following mass parameters were used: ion spray voltage of 3500 V (ESI positive) and −2800 V (ESI negative); turbo spray temperature of 350 °C; ion source temperature of 325 °C; collision energy of 20/40/60 eV; MS and MS/MS scanning range of 100–1500 m/z. Thermo Fisher Scientific (MA, USA) provided Compound Discovery 3.3 and Xcalibur 4.2 software for the MS data analysis. By comparing information from parent ions, MS/MS fragment ions, and full scan mass spectra to those in the database, all chemicals were identified.

Network Pharmacological Analysis

Target Gene Collection of Ingredients in WQY and ACD

After identifying the ingredients in WQY-containing serum, the target genes of these ingredients were obtained from the TCMSP Platform (https://www.tcmsp-e.com/tcmsp.php) and Swiss Target Prediction (http://swisstargetprediction.ch/). In Swiss Target Prediction, the "gene probability" threshold was set to be greater than 0.1. To obtain the target genes of ACD, "allergic contact dermatitis" was used as the search term to search in DrugBank database (https://go.drugbank.com), GeneCards database (https://www.genecards.org), and OMIM database (https://omim.org/). The Venn platform (http://bioinformatics.psb.ugent.be/webtools/Venn/) was utilized to identify genes that overlapped between the target genes of ingredients and the target genes of ACD.

Construction of the Network of Overlapping Genes and Selection of Core Genes

The STRING database (https://cn.string-db.org/) was used to upload the overlapping target genes, specifying the protein type as "Homo sapiens". An interaction score threshold of ≥ 0.900 was applied, resulting in the generation of a PPI network. Cytoscape 3.7.1 (https//cytoscape.org) was utilized for visualizing and analyzing the PPI network. Target genes whose degree value exceeded the median value were selected as the core target genes, and an ingredient–core target gene–ACD network was then built via Cytoscape 3.7.1, in accordance with an aforementioned method.

Pathway Enrichment Analysis

We used the Metascape platform (http://metascape.org/) to conduct Kyoto Encyclopedia of Genes and Genomes (KEGG) and Gene Ontology (GO) analyses on the overlapping core genes. This analysis aimed to investigate the molecular processes that underlie the effects of WQY on ACD. A bubble chart was generated to visualize the relevant KEGG pathways and GO analysis results using a freely available web platform for data analysis (http://www.bioinformatics.com.cn/).

Western Blot Analysis

100 mg ear tissue was lysed on ice for 30 min, and the upper protein extract was obtained via centrifugation. After being separated by 10% sodium dodecyl sulfate polyacrylamide gel electrophoresis, the measured proteins were moved to polyvinylidene fluoride membranes and incubated with primary antibodies against *p*-JAK2 (CST, 3771S), JAK2 (CST, 3230S), *p*-STAT1 (CST, 7649S), STAT1 (CST, 14994S), *p*-p38 (CST, 4631S), p38 (CST, 8690S), *p*-JNK (CST, 4668S), JNK (CST, 9252S), *p*-ERK (CST, 4370S), and ERK (CST, 4695S)for an additional night at 4 °C, followed by a 2-hour incubation (37 °C) with the appropriate peroxidase-conjugated anti-rabbit IgG antibodies. The protein bands were analyzed on a PXi9-TCH imaging analysis system (Syngene, Cambs, UK), and the grayscale values of the proteins were detected and normalized to those of GAPDH.

Serum Metabolites Analysis

100 μL serum samples in each group were used to extract the metabolites, and a Waters ACQUITY ultra-HPLC (Waters, Milford, MA, USA) coupled to an Thermo Q Exactive mass spectrometer system (Thermo Fisher Scientific, MA, USA) was used to examine the samples that were collected.[19,20] Using PCoA in conjunction with multivariate PERMANOVA using Bray-Curtis distances based on relative abundance data computed with the R "vegan" package (v4.3.2), the treatment effect of WQY on serum metabolites was investigated. Phylogenetic tree analysis of Serum metabolites was constructed using cluster_agg of Usearch10 with Bray-Curtis distances. Weighted gene co-expression network analysis (WGCNA) was used to separate the metabolites in mouse serum into modules, and these modules were subsequently connected with the physiological experiment outcomes that performed key functions, such as increases in ear thickness (ETI), increases in ear weight (EWI), serum IgE (SIgE), serum IL-1β (SIL-1β), serum IL-6 (S IL-6), mRNA relative expression of IL-6 (REIL-6), and mRNA relative expression of IL-1β (REIL-1β). The topological overlap matrix, which indicated how similar the common expressions were, was created after the adjacency matrix was first computed using the expression value matrix. The correlation matrix of serum metabolites was transformed into an enhanced adjacency matrix, which followed a scale-free topology with an R2 value of 0.86, achieved by applying a power of r = 6. Hierarchical clustering was applied to the topological overlap matrix to produce clustering trees that together represent the total similarity distribution, and then modules—each given a distinct color—cut the clustering trees that had been produced. Subsequently, each color module's metabolites that demonstrated a strong link with its corresponding index were examined using Venn analysis. Additionally, a study of metabolic pathway enrichment was carried out for the metabolites that were found in each of the six modules.[21]

Statistical Analysis

The mean ± standard deviation (SD) was employed for data representation, with the analysis of all findings being carried out through the utilization of IBM SPSS 20 software (Chicago, IL, USA). Significant differences among the multiple group comparisons were performed using one-way analysis of variance (ANOVA), and the ANOVA comparisons were analyzed through Bonferroni's test when equal variances assumed or Tamhane's T2 test when unequal variances were assumed. A p value < 0.05 indicated significant difference.

Results

Main Compounds in WQY

To ensure the quality of the medicinal materials contained in WQY, we identified and quantified its major components using HPLC. Ten compounds were identified using reference standards, namely gallic acid, chlorogenic acid, geniposide, ferulic acid, jatrorrhizine, baicalin, berberine, wogonoside, baicalein, and wogonin (Figure 1; 1–10, respectively). The contents of seven components with resolutions greater than 1.5 were determined, and their contents were as follows: gallic acid (1), 0.32 $mg \cdot g^{-1}$; jatrorrhizine (5), 2.07 $mg \cdot g^{-1}$; baicalin (6), 19.81 $mg \cdot g^{-1}$; berberine (7), 14.04 $mg \cdot g^{-1}$; wogonoside (8), 6.42 $mg \cdot g^{-1}$; baicalein (9), 0.26 $mg \cdot g^{-1}$; wogonin (10), 0.59 $mg \cdot g^{-1}$.

WQY Attenuated Inflammation and Swelling in Mice with ACD Induced by DNFB

The ear morphology of the mice with ACD was evaluated 24 hours after the last challenge, and ear thickness and weight increases were measured and calculated. The right ear of ACD mice showed remarkable redness, edema, and hypertrophy as shown in Figure 2A, and the increases in ear thickness and weight (0.18 mm and 1.85 mg) were significantly higher when compared to the control group (0.01 mm and 0.09 mg) ($P < 0.01$; $P < 0.01$) (Figure 2B and C). After the oral administration of WQY, the redness and edema in sensitized ears of mice were relieved incredibly, and the ear thickness and weight increases were reduced substantially. The ear thickness and weight increases were significantly reduced in the WQY-L group to 0.13 mm and 1.13 mg, respectively, compared to the model group. Similarly, the WQY-H group likewise displayed significant reductions to 0.07 mm and 0.74 mg.

WQY Alleviated Histopathological Damage in the Ears of ACD Mice Induced by DNFB

Figure 2D illustrates the results of HE staining of the ears of DNFB-induced ACD mice. The mice in the model group displayed a notable thickening of the ear tissue in both the dermal and epidermal layers as compared to the control group, and the intercellular edema, dermal vascular dilation, and infiltration of inflammatory cells were also observed. After administering WQY orally, the ear injuries were greatly alleviated, with noticeable reductions in the thickness of the epidermis and dermis, and a reduction in inflammatory cells, particularly in the WQY-H groups. Meanwhile, the number of mast cells in the ear tissue of the model group of mice increased noticeably, but it was reduced considerably after the oral administration of WQY, especially in the WQY-H groups (Figure 2E).

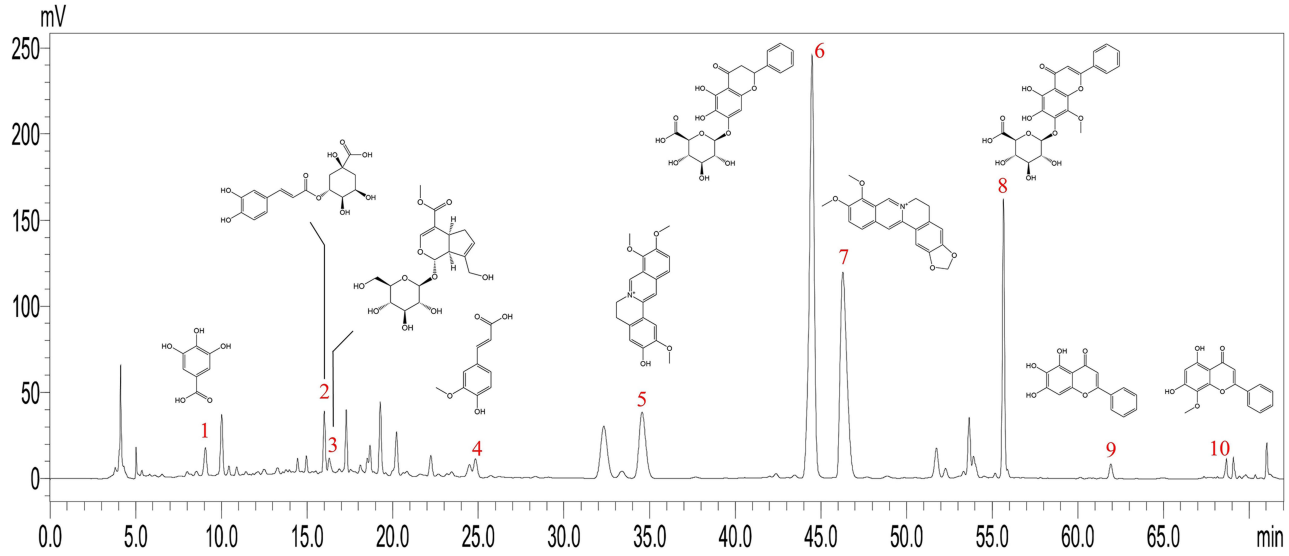

Figure 1 HPLC chromatogram of WQY.

https://doi.org/10.2147/JIR.S512868

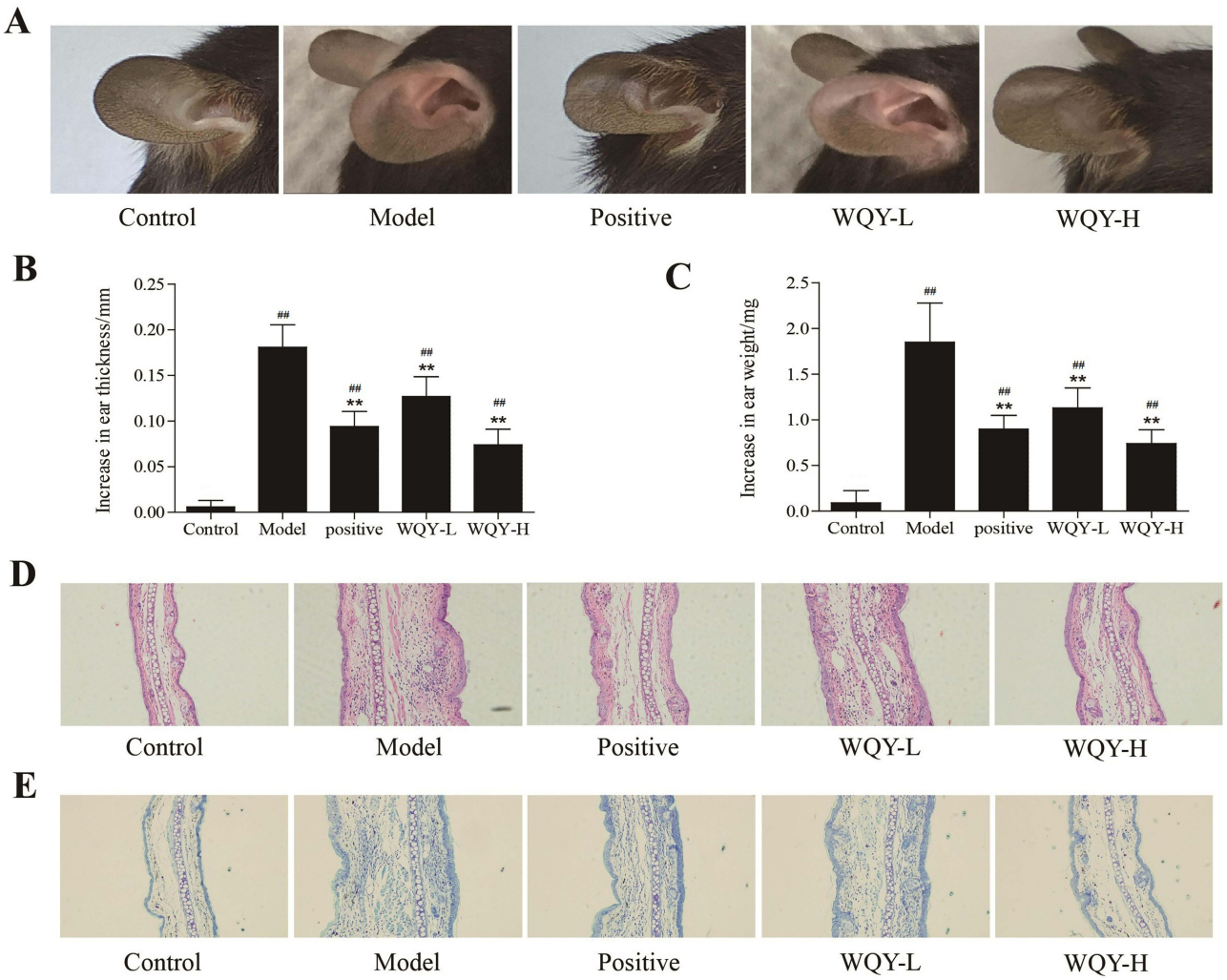

Figure 2 Impact of WQY on the ear inflammation and swelling in mice with DNFB-induced ACD. At 24 h after the last challenge, the ear morphology (**A**) of ACD mice was observed, the ear thickness (**B**) and weight (**C**) increases were measured and calculated. The histopathological injuries in ear samples of mice were observed using HE (**D**) and TB (**E**) stains. Data are expressed as mean ± SD; $n = 10$; ##$P < 0.01$ versus the control group; **$P < 0.01$ versus the model group.

WQY Decreased the Levels of Inflammatory Cytokines in the Sera of DNFB-Induced ACD Mice

The model group's levels of IgE, IL-1β, and IL-6, as depicted in Figure 3, were significantly greater than those of the control group, with values of 88.89 ng/mL, 247.53 pg/mL, and 145.55 pg/mL, respectively. Following the oral administration of WQY, the levels of IgE and IL-1β significantly decreased in both the WQY-L and WQY-H groups, and the levels of IL-6 substantially decreased in the WQY-L and WQY-H groups.

Impact of WQY on Th1 and Th2 Cell Proportions in the SMCs of Mice with DNFB-Induced ACD

Given that ACD is considered to be primarily mediated by antigen-specific Th1 and Th2 cells, the percentages of the two cells in SMCs from mice with ACD were measured and analyzed. As shown in Figure 4, the Th1 cell proportions were significantly higher in the model group (4.86%) compared to the control group (1.80%). Contrarily, there was no notable disparity observed in the Th2 cells of the control and model groups. Following WQY's oral administration, the Th1 cells proportions in the positive, WQY-L, and WQY-H groups were significantly reduced to 2.90%, 3.82%, and 2.48%, whereas those of Th2 cells still did not a significant difference.

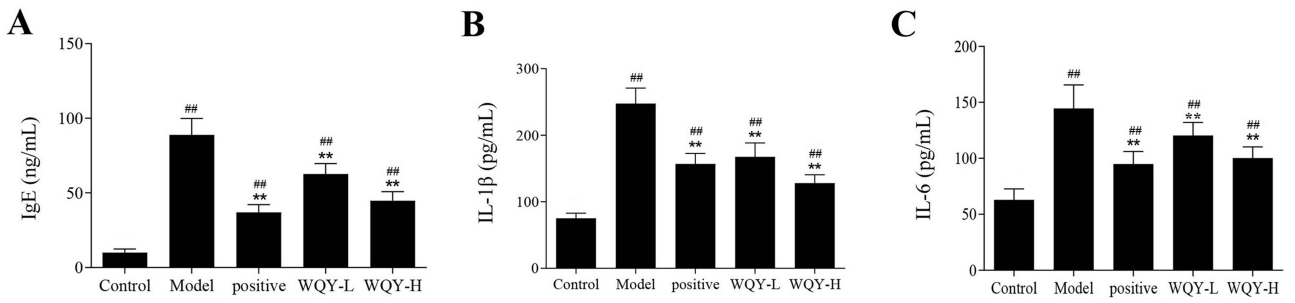

Figure 3 Impact of WQY on the IgE (**A**), IL-1β (**B**), and IL-6 (**C**) levels in serum of mice with DNFB-induced ACD. The blood samples from eyeball of ACD mice were drawn and centrifugated to obtain the serums at 24 hours after the last challenge, the IgE, IL-1β, and IL-6 levels were detected by ELISA. Data are expressed as mean ± SD; $n = 10$; ##$P < 0.01$ versus the control group; **$P < 0.01$ versus the model group.

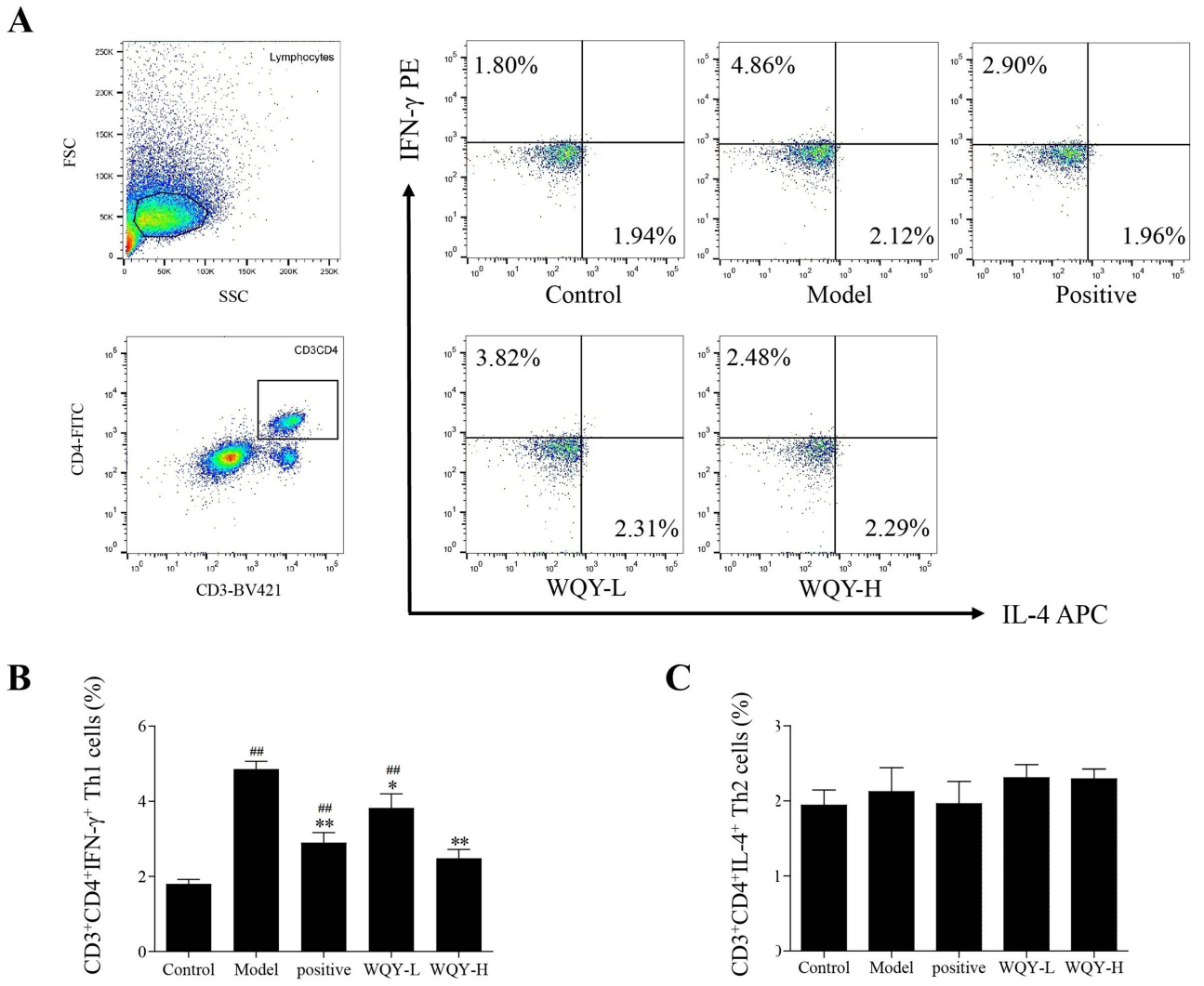

Figure 4 Impact of WQY on Th1 and Th2 cell proportions in the SMCs of mice with DNFB-induced ACD. Th1 and Th2 cells representative dot plots (**A**), the Th1 cells (**B**) and Th2 cells (**C**) proportions in SMCs were detected and analyzed using flow cytometry. Data are expressed as mean ± SD; $n = 3$; ##$P < 0.01$ versus the control group; *$P < 0.05$, **$P < 0.01$ versus the model group.

https://doi.org/10.2147/JIR.S512868

Impact of WQY on the IL-6, IL-1β, IFN-γ, and IL-4 mRNA Levels in the Ears of ACD Mice

To investigate how WQY affects Th1 and Th2 immune cytokines as well as the generation of inflammatory mediators in ACD mice, we measured the IL-6, IL-1β, IFN-γ, and IL-4 mRNA levels in ear tissues via qRT–PCR. As depicted in Figure 5A and B, the IL-6 and IL-1β (inflammatory mediators) mRNA levels in the model group were significantly higher compared to the control group. The mRNA levels of IL-1β and IL-6 in the WQY-L and WQY-H groups showed significant reductions when compared to the model group. WQY-H showed a more superior effect when compared to the positive control group. As illustrated in Figure 5C and D, in the model group, there was a noteworthy rise in mRNA levels of IFN-γ (primarily released by Th1 cells) and IL-4 (primarily released by Th2 cells) compared to the control ($P < 0.01$; $P < 0.01$). After the oral administration of WQY, the IFN-γ levels in the WQY-L and WQY-H groups and IL-4 level in the WQY-H groups were decreased substantially.

Impact of WQY on the T-Bet, GATA3, STAT1, and STAT6 mRNA Levels in the Ears of ACD Mice

It is commonly known that the JAK/STAT signaling pathway plays a part in Th1 and Th2 immune responses.[22,23] To investigate the activity of JAK/STAT pathway, the mRNA levels of key genes, including T-bet, GATA3, STAT1, and STAT6, were quantified using qRT–PCR. In comparison to the control group, the T-bet and STAT1 mRNA levels were significantly greater in the model group as shown in Figure 5E and G. WQY-L and WQY-H application significantly reduced the T-bet and STAT1 mRNA levels in ACD mice. Nevertheless, there were no notable disparities identified in the GATA3 and STAT6 mRNA levels within each group, as depicted in Figure 5F and H.

Components in the Serum Containing WQY

To investigate the possible molecular underpinnings and mode of action of WQY in ACD therapy, we analyzed and identified the ingredients of WQY-containing serum. Figure 6A and B display the total ion chromatograms under positive and negative ion modes of WQY-containing serum acquired using UPLC–MS/MS, respectively. A tentative identification was made for a total of 38 compounds, with 23 detected in positive and 15 detected in negative ion mode, respectively. Table 1 lists all 38 of the discovered constituents in detail, including mass error, ion mode, retention duration, molecular formula, and MS/MS fragmentation.

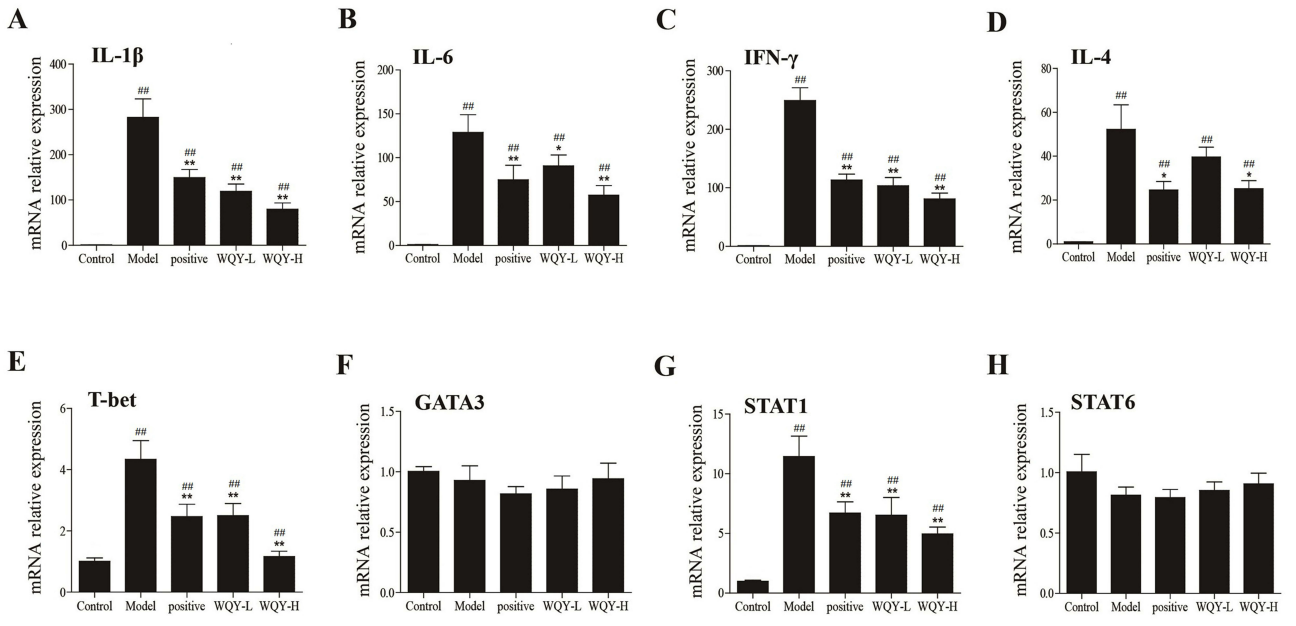

Figure 5 Impact of WQY on the IL-1β (**A**), IL-6 (**B**), IFN-γ (**C**), IL-4 (**D**), T-bet (**E**), GATA3 (**F**), STAT1 (**G**), and STAT6 (**H**) mRNA levels in the ears of mice with ACD. At 24 h after the last challenge, the ear tissues of ACD mice were collected and the mRNA expression levels were measured by qRT–PCR. Data are expressed as mean ± SD; $n = 6$; $^{\#\#}P < 0.01$ versus the control group; $^{*}P < 0.05$, $^{**}P < 0.01$ versus the model group.

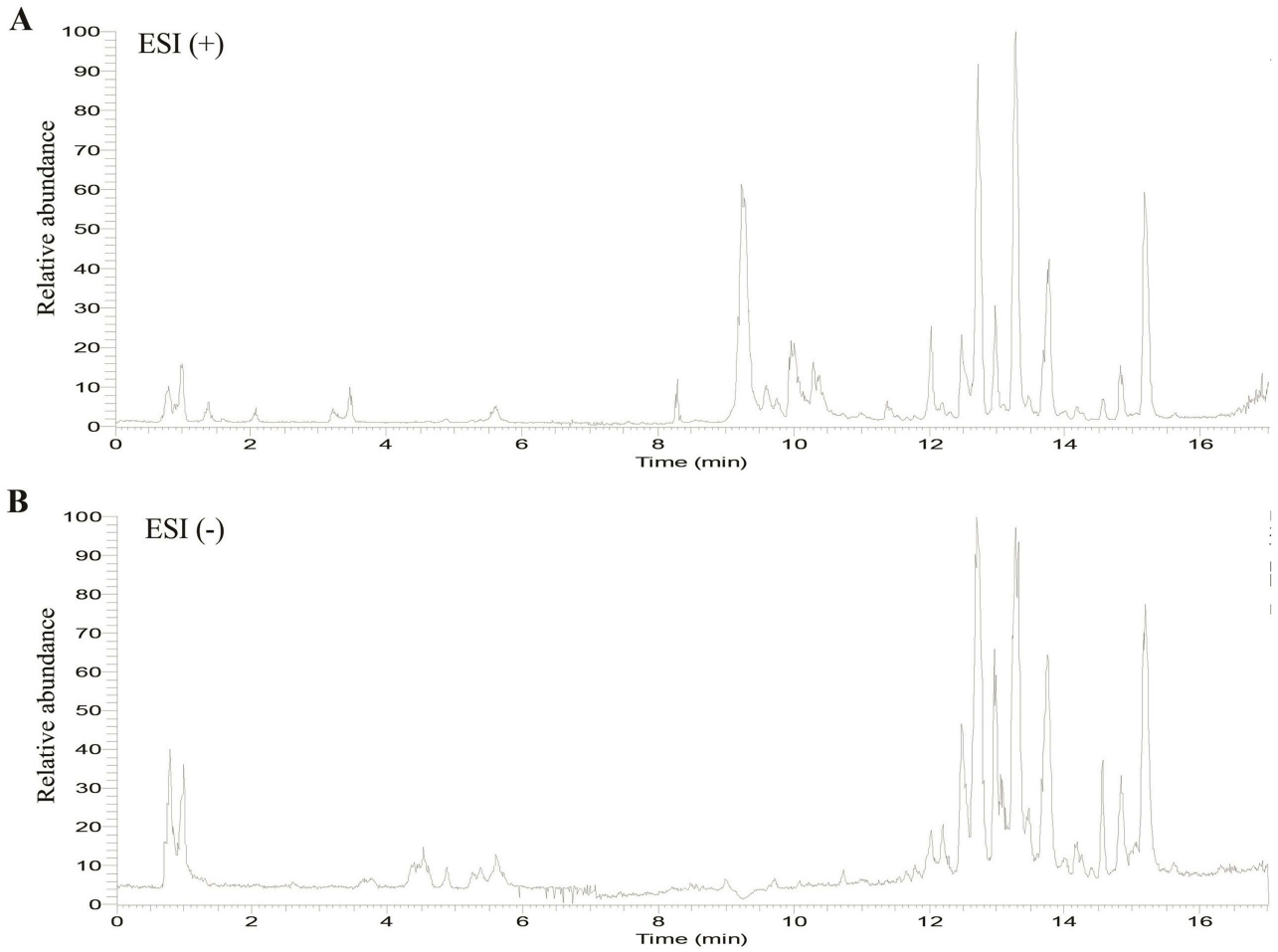

Figure 6 The total ion chromatograms of serum containing WQY in positive (**A**) and negative (**B**) ion modes by UPLC–MS/MS.

Core Target Genes and Potential Pathway Signals of WQY in the Treatment of ACD

Network pharmacological analysis was conducted to further explore the mechanism of WQY in ACD treatment. The Venn diagram in Figure 7A shows that 313 target genes of the ingredients of WQY-containing serum and 1464 target genes of ACD were obtained, and 123 overlapping target genes were identified. The PPI network of the 123 target genes that overlap was analyzed and visualized using Cytoscape 3.7.1 software (Figure 7B). A total of 34 target genes whose degree value exceeded the median value (6.92) were selected as the core target genes, and 16 ingredients closely related to the core targets were considered potential functional components (oxoglaucine, diosmetin, quercetin, berberrubine, wogonin, 1,4-naphthoquinone, apigenin 7-glucuronide, baicalin, hispidulin 7-glucuronide, oroxylin A-7-O-β-D-glucuronide, wogonoside, geniposide, azelaic acid, comanthoside B, DL-arginine, and dihydrooroxylin A). As illustrated in Figure 7C, an ingredient–core target gene–ACD network was then built by importing the core targets, disease, and potential functional components into Cytoscape 3.7.1 software. Results of GO and KEGG pathway enrichment studies for the core target genes are shown in Figure 7D and E, respectively. WQY demonstrates potential in treating ACD by modulating protein phosphorylation, positive regulation of phosphorylation, and affecting key signaling pathways like phosphatidylinositol-3 kinase-Akt, JAK-STAT, and mitogen-activated protein kinase (MAPK) signaling pathways. WQY also might affect various biological processes through its modulation of protein kinase activity, phosphotransferase activity, phosphatase binding, and kinase binding.

https://doi.org/10.2147/JIR.S512868

Table 1 38 Ingredients in WQY-Containing Serum Identified by UPLC-MS/MS

Peak No.	RT (min)	$[M-H]^-$ (m/z)	$[M+H]^+$ (m/z)	Molecular Formula	Error (ppm)	Major MS/MS Fragmentation (m/z)	Assigned Identification
1	0.78	/	175.1189	$C_6H_{14}N_4O_2$	−0.11	158.0928, 116.0706, 70.0653	DL-Arginine
2	0.99	/	262.1285	$C_{11}H^{19}NO_6$	0.17	244.1178, 216.1231, 198.1127	Lotaustralin
3	1.00	111.0086	/	$C_5H_4O_3$	−1.05	67.0191	3-Furoic acid
4	1.00	117.0192	/	$C_4H_6O_4$	−1.02	99.0090, 73.0297	Succinic acid
5	1.22	373.1136	/	$C_{16}H_{22}O_{10}$	−1.13	211.0621, 149.0614, 123.0457	Geniposidic acid
6	1.50	/	220.1180	$C_9H_{17}NO_5$	−0.23	202.1070, 90.0548	pantothenic acid
7	1.75	/	209.0808	$C_{11}H_{12}O_4$	−0.02	191.0704, 149.0599, 105.0700	3,4-Dimethoxycinnamic acid
8	2.59	/	121.0648	C_8H_8O	0.33	105.0448, 93.0699	Acetophenone
9	2.90	/	462.1762	$C_{23}H_{27}NO_9$	0.68	286.1435, 228.9120	Hydromorphone 3-Glucuronide
10	3.08	203.0822	/	$C_{11}H_{12}N_2O_2$	−0.89	186.0570, 142.0668, 116.0510	DL-Tryptophan
11	3.60	/	462.1762	$C_{23}H_{27}NO_9$	0.65	417.4519, 286.1437, 228.9227, 107.0491	Morphine-3-glucuronide
12	4.24	193.0505	/	$C_{10}H_{10}O_4$	−0.63	172.0272, 134.0378	Isoferulic acid
13	4.74	167.0349	/	$C_8H_8O_4$	−0.56	123.0452	Homoprotocatechuic acid
14	4.88	/	191.0703	$C_{10}H_6O_2$	0.05	159.0441, 131.0492	1,4-Naphthoquinone
15	4.88	433.1346	/	$C_{17}H_{24}O_{10}$	−1.12	225.0773, 101.0246	Geniposide
16	5.15	/	342.1701	$C_{20}H_{23}NO_4$	0.28	297.1122, 265.0858, 58.0653	Magnoflorine
17	5.95	163.0400	/	$C_9H_8O_3$	−0.4	119.0504	3-Coumaric acid
18	5.95	/	147.0441	$C_9H_6O_2$	0.6	119.0491, 51.0541	Coumarin
19	6.46	/	195.0652	$C_{10}H_{10}O_4$	−0.12	177.0546, 134.0340, 117.0335, 89.0387	Ferulic Acid
20	6.54	/	190.0500	$C_{10}H_7NO_3$	0.47	172.0394	Kynurenic acid
21	6.60	301.0353	/	$C_{15}H_{10}O_7$	−0.17	151.0043, 125.0248	Quercetin
22	6.73	/	322.1075	$C_{19}H_{15}NO_4$	0.22	307.0840, 279.0886	Berberrubine
23	7.17	/	146.0601	C_9H_7NO	0.31	118.0651, 91.0542	8-Hydroxyquinoline
24	7.43	187.0975	/	$C_9H_{16}O_4$	−0.3	169.0869, 143.1078, 123.0815	Azelaic acid
25	7.84	445.0774	/	$C_{21}H_{18}O_{11}$	0.05	269.0461, 203.0872	apigenin 7-glucuronide
26	8.27	/	191.1066	$C_{12}H_{14}O_2$	−0.1	149.0598, 105.0698	Ligustilide
27	8.42	459.0932	/	$C_{22}H_{20}O_{11}$	0.26	268.0380, 113.0246	Oroxylin A-7-O-β-D-glucuronide
28	8.48	/	477.1030	$C_{22}H_{20}O_{12}$	0.62	301.0708, 286.0474	Hispidulin 7-glucuronide
29	8.56	445.0774	/	$C_{21}H_{18}O_{11}$	0.09	269.0460, 203.0867	Baicalin
30	8.65	/	461.1082		0.18	285.0757, 270.0522, 252.0433	Wogonoside
31	8.81	/	287.0914	$C_{16}H_{14}O_5$	0.08	183.0290, 168.0060	Dihydrooroxylin A
32	8.93	489.1037	/	$C_{23}H_{22}O_{12}$	0.33	313.0721, 203.0869	Comanthoside B
33	9.56	299.0560	/	$C_{16}H_{12}O_6$	−0.03	284.0327, 203.0872	Diosmetin
34	10.94	/	285.0759	$C_{16}H_{12}O_5$	0.34	270.0519, 224.0455	Wogonin
35	11.13	/	352.1180	$C_{20}H_{17}NO_5$	0.32	322.0710, 294.0749	Oxoglaucine
36	11.67	/	300.2898	$C_{18}H_{37}NO_2$	0.22	282.2792	D-Sphingosine
37	13.24	/	400.3424	$C_{23}H_{45}NO_4$	0.66	341.2688, 239.2369, 85.0284	Palmitoylcarnitine
38	16.83	/	359.3158	$C_{21}H_{42}O_4$	0.84	341.3040	Glyceryl monostearate

Abbreviations: RT, Retention time; m/z, mass-to-charge ratio.

WQY Suppressed the JAK/STAT and MAPK Signaling Pathways in ACD Treatment

Several studies have indicated the critical involvement of the JAK/STAT and MAPK signaling pathways in ACD.[24,25] Based on a previous network pharmacological analysis, the effect of WQY on the expressions of proteins related to the JAK/STAT and MAPK pathways in DFNB-induced ACD mice was measured. In the model group, the expression ratios

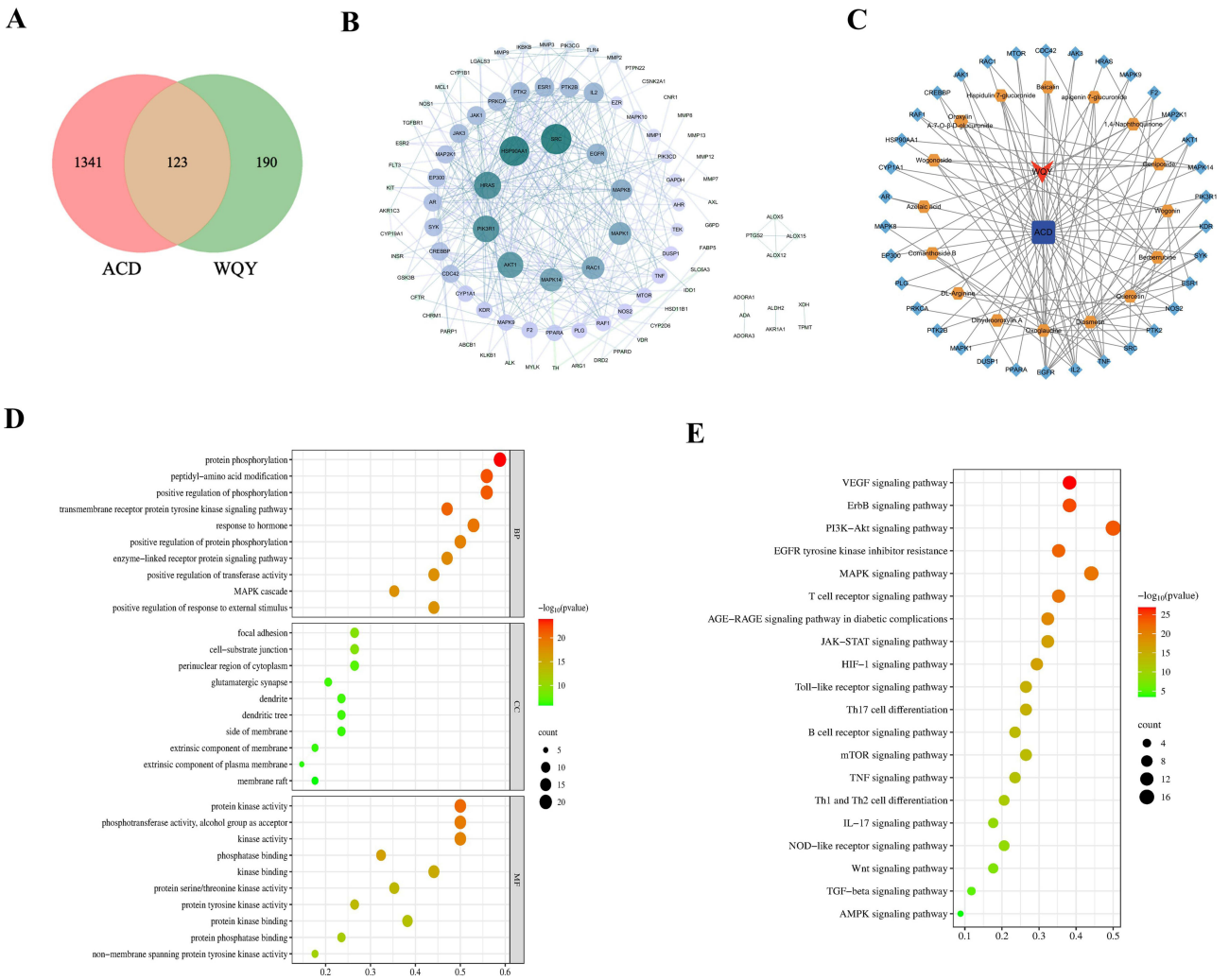

Figure 7 Predicted target genes and pathway signals of WQY in the treatment of ACD via network pharmacological analysis. Venn diagram of common overlapping targets of WQY and ACD (**A**). PPI network of the 123 overlapping target genes of WQY and ACD (**B**). Ingredient–core target gene–ACD network (**C**), GO (**D**) and KEGG (**E**) pathway enrichment dot-plot diagrams of WQY in the treatment of ACD.

of *p*-JAK2 to JAK2 and *p*-STAT to STAT1 were significantly higher compared to the control group as shown in Figure 8A and B. After taking WQY orally, the WQY-H group showed a significant decrease in the ratio of p-JAK2 to JAK2, while both the WQY-L and WQY-H groups exhibited a significant decrease in the ratios of *p*-JAK2 to JAK2 and *p*-STAT to STAT1. As seen in Figure 8C, there were significantly rises in the expression ratios of *p*-ERK to ERK, *p*-JNK to JNK, and *p*-p38 to p38 in the model group when compared to the control group. The application of WQY-L led to a significant inhibition of the increased ratios of *p*-ERK/ERK and *p*-p38/p38, while WQY-H significantly inhibited the increased levels of *p*-ERK/ERK, *p*-JNK/JNK, and *p*-p38/p38 ratios. These results show that WQY depressed the JAK/STAT and p38-MAPK signaling pathways activation in DNFB-induced ACD mice.

Impact of WQY on Serum Metabolites During the Treatment of ACD

As shown in Figure 9A and B, the model and control groups' relative metabolite contents differed markedly from those of the positive, WQY-L, and WQY-H groups. In the Bray-Curtis distance PCoA over all samples, the two-dimensional points of positive, WQY-L, and WQY-H groups clustered together, which revealed that their serum metabolites were relatively similar. Meanwhile, the two-dimensional points of control and model groups clustered into different branches, which showed high difference. In this study, a co-expression network was built using the R software's WGCNA package. 4318 serum metabolites with an average relative abundance greater than 0.5 were chosen to build the co-expression network based on the relative

https://doi.org/10.2147/JIR.S512868

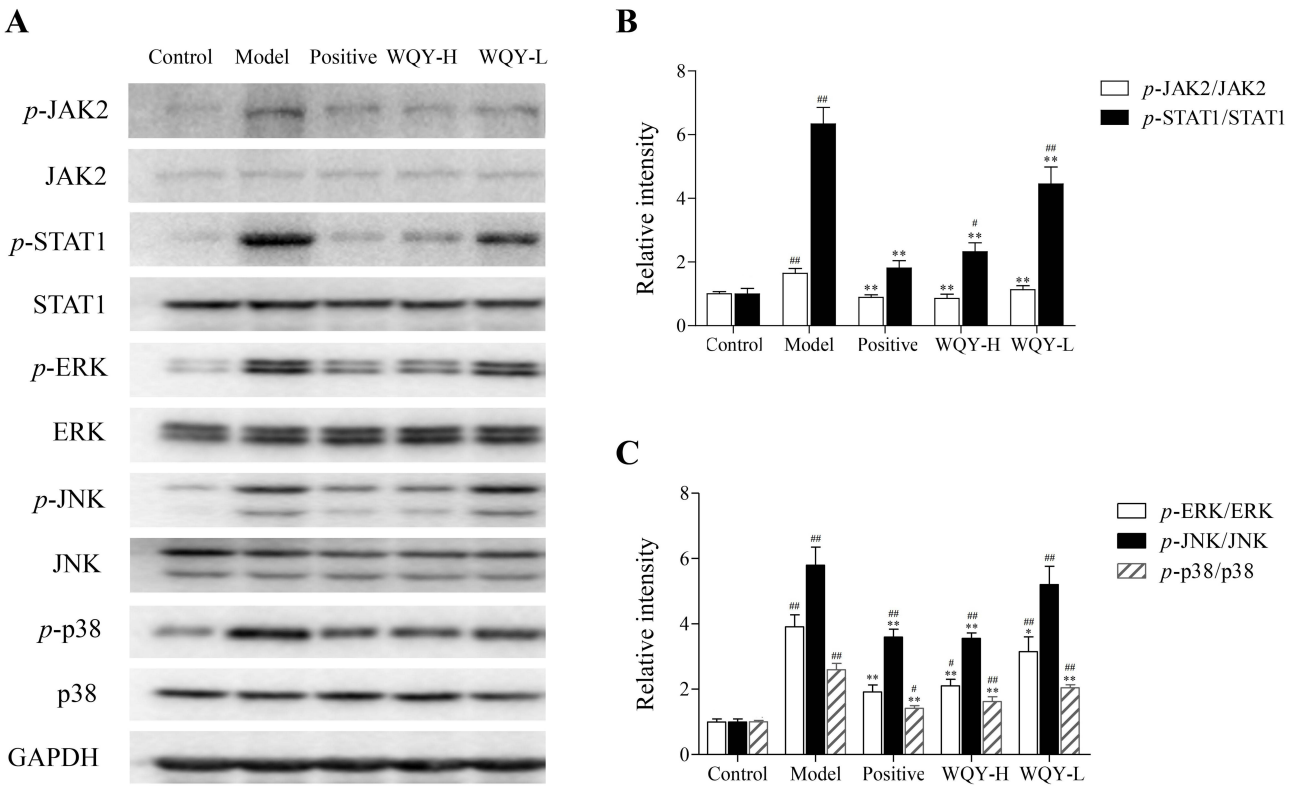

Figure 8 Impact of WQY on the JAK/STAT and MAPK signaling pathways in DFNB-induced ACD mice. At 24 h after the last challenge, the ear tissues of ACD mice were removed. The extracted proteins were quantified and separated by 10% SDS-PAGE, and the *p*-JAK2, JAK2, *p*-STAT1, STAT1, *p*-p38, and p38, *p*-JNK, JNK, *p*-ERK, and ERK expressions (**A**) were measured by Western blotting. Next, the analysis focused on the ratios of p-JAK2 to JAK2 and p-STAT to STAT1 (**B**), as well as the ratios of p-ERK to ERK, p-JNK to JNK, and p-p38 to p38 (**C**). Data are expressed as mean ± SD; $n = 3$; ##$P < 0.01$, #$P < 0.05$ versus the control group; *$P < 0.05$, **$P < 0.01$ versus the model group.

abundance data. Six co-expression modules for serum metabolites were found after the scale-free network was constructed using the physiological experimental data (ETI, EWI, SIgE, SIL-1β, SIL-6, REIL-1β, and REIL-6) that had previously been gathered, and 7 physiological indicators had significant positive correlations with MEdarkgreen among them ($R > 0.7$, $P < 0.01$, Figure 9C). The metabolites in each color module that were significantly correlated with the corresponding index were analyzed by Venn analysis, and 205 metabolites were found to be present in all six modules (Figure 9D). A total of 205 metabolites were subjected to enrichment analysis of metabolic pathways, resulting in the identification of 25 metabolic pathways as illustrated in Figure 9E, such as methylhistidine metabolism, nicotinate and nicotinamide metabolism, methionine metabolism, tryptophan metabolism, and phosphatidylcholine biosynthesis.

Discussion

ACD is a hypersensitivity disease that is characterized by delayed immune responses and is mediated by antigen-specific T cells, specifically Th1 and Th2 cells. During the sensitization phase of ACD, allergens provoke the release of various cytokines, including IL-1α, IL-1β, tumor necrosis factor-α, and IL-8, by keratinocytes. This, in turn, leads to vasodilation, the recruitment of immune cells, and the infiltration of the affected region.[26] Langerhans and dermal dendritic cells expose allergens to the lymph nodes that are connected, resulting in the activation of hapten-specific T cells, including Th1, Th2, Th17, and regulatory T cells.[26] When individuals are exposed to allergens during the elicitation phase, the hapten-specific T cells, along with mast cells and eosinophils, undergo proliferation, subsequently migrate to the initial contact site, and release inflammatory factors, which eventually result in skin inflammation.[27] Currently, the existing anti-ACD drugs in Western medicine, such as corticosteroids and immunosuppressants, can cause a series of adverse reactions.[3–5] Therefore, studies should focus on the search for TCM with reliable efficacy and minimal side effects to treat ACD.

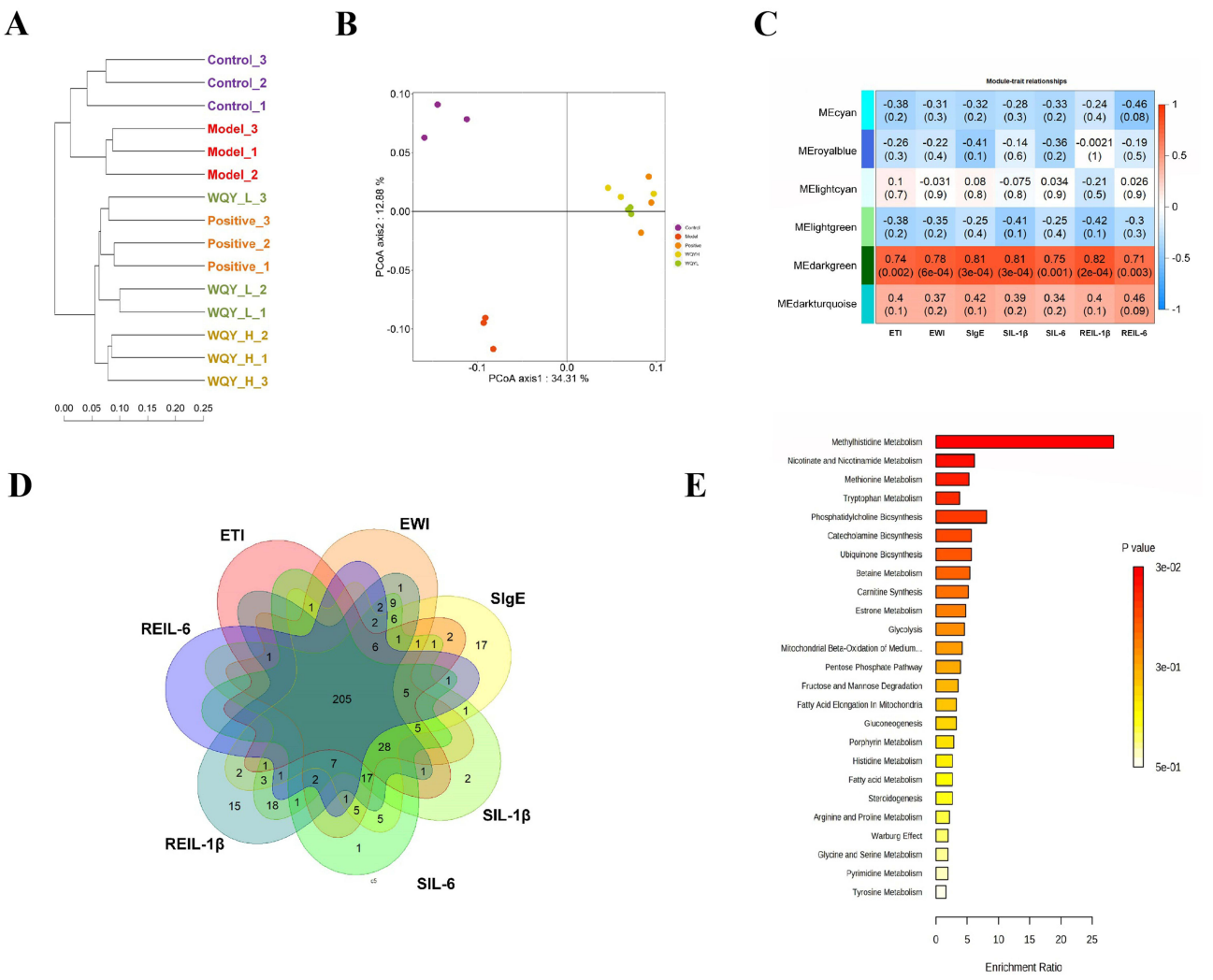

Figure 9 Impact of WQY on serum metabolites in ACD mice induced by DFNB. Bray–Curtis distance clustering (**A**) and two-dimensional ranking of PCoA analysis (**B**) (P-value = 0.01, R2 = 0.46) of serum metabolites. Mouse serum metabolites were divided into modules by using WGCNA analysis, then correlated with the physiological experiment results that performed key functions, such as increases in ear thickness (ETI), increases in ear weight (EWI), serum IgE (SIgE), serum IL-1β (SIL-1β), serum IL-6 (S IL-6), mRNA relative expression of IL-1β and IL-6 (REIL-1β and REIL-6). Relationships between various color modules and blood metabolites based on physiological experiment outcomes (**C**). Venn diagram of serum metabolites in each color module (**D**). Physiological metabolic pathways enriched by 205 common metabolites (**E**).

WQY is a classic prescription derived from the ancient medical book Wanbing Huichun, and it is commonly used to treat ACD, chronic eczema, and canker sore in Asian countries, especially in Japan.[8–11] In this work, a DNFB-induced typical ACD mouse model was adopted to conduct a systematic and comprehensive investigation on the therapeutic effect and mechanism of WQY in ACD treatment for the first time. The findings demonstrate that WQY effectively reduced redness and swelling in sensitized ears of ACD mice, as well as decreased epidermal and dermal thickness, basophil infiltration, and mast cell proliferation in the ear tissue. Originating from hematopoietic stem cells, mast cells are extensively present in epidermal tissues and play a crucial role as effector cells in the development of ACD.[28,29] Mast cells are pivotal in promoting contact hypersensitivity through the adjuvant effects of haptens, and this early inflammatory response enhances T cell reactivity to the hapten via multiple mechanisms, including facilitating the migration of dendritic cells from hapten-exposed skin to draining lymph nodes.[28] In addition, WQY considerably reduced the increases in ear thickness and weight, reduced the IgE, IL-1β, and IL-6 levels in the serums and downregulated the IL-6 and IL-1β (inflammatory cytokines) mRNA levels in the ears of mice with ACD. The aforementioned findings collectively demonstrate that WQY plays a crucial role in ACD treatment. In consideration of the important role of Th1 and Th2 cells in the pathogenesis of ACD, Th1 and Th2 immune responses have been evaluated. The results of this

experiment showed a considerable decrease in the mRNA levels of Th1- and Th2-released IFN-γ and IL-4 in the ears. Additionally, WQY also reduced the Th1 cells percentages in SMCs of ACD mice. The results demonstrate that the Th1 immune response was considerably enhanced in DNFB-induced ACD mice and WQY can suppress the Th1 response. IL-4 is a crucial cytokine at the effector stage of contact hypersensitivity reaction, and it is highly expressed in ACD lesions.[30,31] The most crucial cells for IL-4 secretion are Th2 cells. However, many other cell types, such as mast cells and basophils can also produce IL-4. IL-4 was identified as the first cytokine to be produced by mast cells and is responsible for stimulating and maintaining the allergic inflammatory response.[32,33] In this study, no significant differences in Th2 cell frequencies were observed between groups. However, mice with ACD showed markedly increased IL-4 production and enhanced mast cell accumulation in the ears relative to the control group, indicating that mast cells may be the main effector cells for IL-4 production in ACD mice. Our findings demonstrate that WQY-mediated suppression of IL-4 secretion in ACD mice is likely attributable to a reduction in mast cell infiltration rather than inhibition of Th2 cell differentiation.

The significance of the JAK/STAT signaling pathway in Th1 and Th2 immune responses should not be underestimated.[23] When released IFN-γ binds to its receptor, the JAK/STAT1 signal transduction pathway activates and expresses the T-bet gene. Moreover, the presence of T-bet enhances the differentiate of Th0 cells into Th1 cells.[22] The transcription factor GATA3 is activated when IL-4 attaches to its receptor, which causes the activation of STAT6. According to Zeng, this condition enables the conversion of Th0 cells to Th2 cells and the release of Th2 cytokines.[34] To evaluate the mechanism of WQY in ACD treatment, we assessed the T-bet, GATA3, STAT1, and STAT6 levels in relation to the JAK/STAT pathway for preliminary research. WQY reduced substantially the T-bet and STAT1 mRNA levels in the ears of ACD mice, whereas there were no discernible variations in the GATA3 and STAT6 levels. The results findings indicate that WQY can inhibit the Th1 immune response by targeting the JAK/STAT1 signaling pathway in the management of ACD.

To further investigate the potential active ingredients and mechanism of WQY in the treatment of ACD, we performed UPLC–MS/MS and network pharmacological analyses. Given the complexity of the components and targets of TCM formulations, they can be analyzed using network pharmacological technology from a holistic perspective.[35] Lin employed network pharmacology to examine the active constituents of 78 frequently used TCM herbs for lowering blood glucose levels, resulting in the successful identification of several small molecules that boasted comparable drug properties to existing Western medications.[36] In this study, 38 ingredients of WQY-containing serum were identified by UPLC–MS/MS, and 123 overlapping target genes of WQY and ACD were obtained. The analysis of 34 core target genes, out of 123, using GO and KEGG enrichment, suggests that WQY may have potential in treating ACD by modulating specific biological processes, such as the JAK-STAT and MAPK signaling pathways. Given the key role of the JAK/STAT signaling pathway in skin inflammation, therapeutic utilization of JAK/STAT inhibitors has been effective to treat inflammatory skin diseases, including contact hypersensitivity.[37,38] *Ke-teng-zi* plays a therapeutic role in ACD via the JAK/STAT3 signaling pathway, and *Sanguisorbae Radix* reduces the inflammatory response by inhibiting JAK2/STAT1 activation in bone marrow-derived mast cells.[24,39]

The MAPK signaling pathway is important in regulating the expression of proinflammatory genes and initiating the inflammatory response, and among the different subtypes of MAPKs, JNK, ERK, and p38 MAPK are considered essential.[40] Various studies have shown that the MAPK signaling pathway is evidently activated in the skin lesions of ACD animals.[41,42] In addition, the activation of the MAPK pathway increases the secretion of IL-4 in mast cells.[43] Accordingly, combining the previous experimental results, the expression levels of proteins in relation to the MAPK and JAK/STAT1 signaling pathways were detected. According to the findings, it is suggested that WQY reduced the *p*-JAK2, *p*-STAT3, *p*-ERK, *p*-JNK, and *p*-p38 levels in the ears of ACD mice, which inhibited the MAPK and JAK2/STAT3 signaling pathways activation in ACD treatment.

In this study, a total of 16 constituents were considered to be the potential functional components of WQY in the treatment of ACD, and the top ranked substances in WQY were oxoglaucine, diosmetin, quercetin, and berberrubine, and wogonin. Diosmetin and quercetin have been found to significantly decrease the IgE and IL-4 levels in serum of mice with DNCB-induced atopic dermatitis and contact hypersensitivity, and these compounds were also found to decrease the IL-4 mRNA level in RBL-2H3 cells.[44,45] In addition, it was also demonstrated that diosmetin can inhibit the phosphorylation of MAPK as well as the JAK/STAT signaling pathways activation in IL-4-induced raw 264.7 cells.[46] Wogonin, which acts as a suppressor of cyclooxygenases-2, demonstrated notable anti-inflammatory effects in mice with contact dermatitis, leading to a reduction in the IL-1β, IFN-γ, intercellular adhesion molecule-1 levels in the ears.[47] Wogonin was

also proven to inhibit the JAK2/STAT1/2 signaling pathway activation in the human chondrocyte cell line SW1353 stimulates with IL-1β.[48] Therefore, it can be seen that the selected ingredients above are likely to be the ingredients in action of WQY to treat ACD, and they merit further investigation in subsequent studies.

Furthermore, the serum metabolites of WQY in the treatment of ACD were also examined. Metabolic activity is the material basis for maintaining life in organisms, and the analysis of metabolites is an important aspect of studying the molecular basis of life activity. 25 metabolic pathways were obtained and considered to have a potential impact on the treatment of ACD with WQY in this study, such as methylhistidine metabolism, nicotinate and nicotinamide metabolism, methionine metabolism, tryptophan metabolism, and phosphatidylcholine biosynthesis. Nicotinamide, the biologically active form of vitamin B3, is essential for over 200 enzymatic reactions within the body, including the production of ATP. Numerous skin conditions, such as rosacea, nonmelanoma skin cancer, and atopic dermatitis, have been demonstrated to respond well to topical nicotinamide therapy.[49] In a mouse model, selenium-L-methionine was also studied and found to have a significant impact on chronic inflammatory skin disease.[50] Similar to other essential amino acids, tryptophan also generates metabolites that bind to the aryl hydrocarbon receptor (AHR) and helps regulate the immune system in the intestines and skin, and these metabolites have interactions with dendritic cells and innate lymphoid cells, among other immune cells.[51] *Bifidobacterium longum* has been shown to alleviate atopic dermatitis through the gut-skin axis by facilitating the metabolism of tryptophan through the AHR signaling pathway.[52] Currently, there have been limited research on the in vivo metabolism of ACD medication treatment, further research is needed on the specific biological role of metabolic activity in the treatment of ACD with WQY.

In addition, as a classical TCM formulation capable of simultaneously exerting both "warming" and "clearing" therapeutic effects, WQY exemplifies the holistic principles of combined herbal medicine in its application for ACD treatment. This dual-action mechanism comprehensively embodies the characteristic integrative approach of traditional Chinese pharmacotherapy. Therefore, future investigations could focus on elucidating the therapeutic principles underlying WQY's combined warming-clearing formulation for ACD treatment, and such research would provide critical experimental evidence to advance scientific understanding of TCM's dual-modality therapeutic approach.

Conclusion

In summary, WQY exhibited a significant anti-inflammatory role on DNFB-induced ACD mice via inhibiting the Th1 immune response and IL-4 secretion. Based on a combination of UPLC–MS/MS, network pharmacological analysis, and Western blot analyses, the mechanism underlying the treatment of ACD by WQY may be tightly correlated with the suppression of MAPK and JAK2/STAT1 signaling pathways. This study presents experimental evidence supporting the clinical application of WQY and the development of novel drugs for treating ACD. Additionally, the projected possible functional components of WQY can be further investigated.

Abbreviations

WQY, Wenqing Yin; ACD, Allergic contact dermatitis; Th1, T helper 1; SMCs, spleen mononuclear cells; DNFB, 2,4-Dinitrofluorobenzene; Th2, T helper 2; TCM, Traditional Chinese medicine; PE, Phycoerythrin; FITC, Fluorescein isothiocyanate; APC, Allophycocyanin; *p*-JAK, Phospho-Janus kinase; ERK, extracellular signal-regulated kinase; STAT, signal transducer and activator of transcription; JNK, c-Jun N-terminal kinase; WQY-H, high-concentration WQY; WQY-L, low-concentration WQY; TB, Toluidine blue; HE, Hematoxylin and eosin; FBS, Fetal bovine serum; cDNA, Complementary DNA; PPI, Protein-protein interaction; AHR, aryl hydrocarbon receptor; PBS, Phosphate-buffered saline.

Funding

This work was support by the National Natural Science Foundation of China (grant number: 82004252) and the Project of Administration of Traditional Chinese Medicine of Guangdong Province (grant number: 20251219).

Disclosure

The authors declare that they have no competing interests in this work.

References

1. Liu BY, Escalera J, Balakrishna S, et al. TRPA1 controls inflammation and pruritogen responses in allergic contact dermatitis. *FASEB J*. 2013;27:3549–3563. doi:10.1096/fj.13-229948
2. Peiser M, Tralau T, Heidler J, et al. Allergic contact dermatitis: epidemiology, molecular mechanisms, in vitro methods and regulatory aspects. Current knowledge assembled at an international workshop at BfR, Germany. *Cell Mol Life Sci*. 2012;9:763–781. doi:10.1007/s00018-011-0846-8
3. Demehri S, Cunningham TJ, Hurst EA, et al. Chronic allergic contact dermatitis promotes skin cancer. *J Clin Invest*. 2014;124:5037–5041. doi:10.1172/JCI77843
4. Nankivell BJ, Borrows RJ, Fung CL, et al. Calcineurin inhibitor nephrotoxicity: longitudinal assessment by protocol histology. *Transplantation*. 2004;78:557–565. doi:10.1097/01.tp.0000128636.70499.6e
5. Prakash AV, Davis MDP. Contact dermatitis in older adults: a review of the literature. *Am J Clin Dermatol*. 2010;11:373–381. doi:10.2165/11319290-000000000-00000
6. Ma TJ. Experience of WANG Wenchun, a famous veteran doctor of traditional Chinese medicine, in treating contact dermatitis. *World Latest Med Info*. 2016;16:128–129. doi:10.3969/j.issn.1671-3141.2016.65.103
7. Lin LS, Mai YZ. TCM treatment of contact dermatitis. *J Changchun Univ Chin Med*. 2010;26:151–152. doi:10.13463/j.cnki.cczyy.2010.01.046
8. Che W. *Clinical Retrospective Summary of Wenqingyin in the Treatment of Atopic Dermatitis [D]*. Beijing, China: Beijing University of Chinese Medicine; 2005.
9. Du X, Liu AM. Research progress on modern pharmacology and clinical application of Wenqingyin. *Chin J Trad Med Sci Tech*. 2008;15:399–400. doi:10.3969/j.issn.1005-7072.2008.05.066
10. Li JF, Zhang GZ. Application of Wenqing Yin in Department of Dermatology. *China Med Abs Derm*. 2017;34:168–173+4.
11. Qin CZ, Shi JS. Clinical study on the treatment of atopic dermatitis with Wenqingyin. *China for Med Treatment*. 2008;55–56. doi:10.16662/j.cnki.1674-0742.2008.12.016
12. Du X, Zhang Y, Li YW, et al. Experimental study on the two-way regulating effect of Wenqingyin on immunity. *J Basic Chin Med*. 1999;5:31–32. doi:10.3969/j.issn.1006-3250.1999.11.010
13. Yu CS, Yang HR, Jiang YH, et al. Effects of Wenqingyin on the proliferation and differentiation of HaCaT cells. *J Eme Trad Chin Med*. 2014;23:2174–2176. doi:10.3969/j.issn.1004-745X.2014.12.011
14. Chen GF, Gao J, Yang WP, et al. The pharmacological effect of *Wumeiwan* on atopic dermatitis mice. *Chin Trad Pat Med*. 2022;44(12):4004–4008. doi:10.3969/j.issn.1001-1528.2022.12.044
15. Si, Tu HJ, Wang Y, et al. Establishment of HPLC fingerprints for Wenqingyin and simultaneous determination of seven constituents. *Chin Trad Pat Med*. 2022;44:3115–3119. doi:10.3969/i.issn.1001-1528.2022.10.006
16. Wang ZG, Yi T, Long M, et al. Involvement of the negative feedback of il-33 signaling in the anti-inflammatory effect of electro-acupuncture on allergic contact dermatitis via targeting MicroRNA-155 in Mast cells. *Inflammation*. 2018;41:859–869. doi:10.1007/s10753-018-0740-8
17. Ren MY, Wang Y, Lin L, et al. α-linolenic acid screened by molecular docking attenuates inflammation by regulating Th1/Th2 imbalance in ovalbumin-induced mice of allergic rhinitis. *Molecules*. 2022;27:5893. doi:10.3390/molecules27185893
18. Pfaffl MW. A new mathematical model for relative quantification in real-time RT-PCR. *Nucleic Acids Res*. 2009;29:e45. doi:10.1093/nar/29.9.e45
19. Demurtas A, Pescina S, Nicoli S, et al. Validation of a HPLC-UV method for the quantification of budesonide in skin layers. *J Chromatogr B*. 2020;1164:122512. doi:10.1016/j.jchromb.2020.122512
20. Want EJ, Masson P, Michopoulos F, et al. Global metabolic profiling of animal and human tissues via UPLC-MS. *Nat Protoc*. 2013;8(1):17–32. doi:10.1038/nprot.2012.135
21. Langfelder P, Horvath S. WGCNA an R package for weighted correlation network analysis. *BMC Bioinform*. 2008;9:559. doi:10.1186/1471-2105-9-559
22. Bowen H, Kelly A, Lee T, et al. Control of cytokine gene transcription in Th1 and Th2 cells. *Clin Exp Allergy*. 2008;38:1422–1431. doi:10.1111/j.1365-2222.2008.03067.x
23. Villarino AV, Kanno Y, Ferdinand JR, et al. Mechanisms of Jak/STAT signaling in immunity and disease. *J Immunol*. 2015;194:21–27. doi:10.4049/jimmunol.1401867
24. Ju YK, Luo M, Yan T, et al. TRPA1 is involved in the inhibitory effect of Ke-teng-zi on allergic contact dermatitis via MAPK and JAK/STAT3 signaling pathways. *J Ethnopharmacol*. 2023;307:116182. doi:10.1016/j.jep.2023.116182
25. Li WH, Liu FX, Wang J, et al. MicroRNA-21-mediated inhibition of mast cell degranulation involved in the protective effect of Berberine on 2,4-Dinitrofluorobenzene-induced allergic contact dermatitis in rats via p38 pathway. *Inflammation*. 2018;41:689–699. doi:10.1007/s10753-017-0723-1
26. Gittler JK, Krueger JG, Guttman-Yassky E. Atopic dermatitis results in intrinsic barrier and immune abnormalities: implications for contact dermatitis. *J Allergy Clin Immunol*. 2013;131:300–313. doi:10.1016/j.jaci.2012.06.048
27. Nosbaum A, Vocanson M, Rozieres A, et al. Allergic and irritant contact dermatitis. *Eur J Dermatol*. 2009;19:325–332. doi:10.1684/ejd.2009.0686
28. Dudeck A, Dudeck J, Scholten J, et al. Mast cells are key promoters of contact allergy that mediate the adjuvant effects of haptens. *Immunity*. 2011;34:973–984. doi:10.1016/j.immuni.2011.03.028
29. Morita H, Saito H, Matsumoto K, et al. Regulatory roles of mast cells in immune responses. *Semin Immunopathol*. 2016;38:27154294. doi:10.1007/s00281-016-0566-0
30. Campos RA, Szczepanik M, Itakura A, et al. Interleukin-4-dependent innate collaboration between iNKT cells and B-1 B cells controls adaptative contact sensitivity. *Immunology*. 2005;117(4):536–546. doi:10.1111/j.1365-2567.2006.02330.x
31. Rowe A, Bunker CB. Interleukin-4 and the interleukin-4 receptor in allergic contact dermatitis. *Contact Dermatitis*. 1998;38:36–39. doi:10.1111/j.1600-0536.1998.tb05634.x
32. Paul WE. History of Interleukin-4. *Cytokine*. 2015;75:3–7. doi:10.1016/j.cyto.2015.01.038
33. McLeod JJA, Baker B, Ryan JJ. Mast cell production and response to IL-4 and IL-13. *Cytokine*. 2015;75:57–61. doi:10.1016/j.cyto.2015.05.019
34. Zeng WP. 'All things considered': transcriptional regulation of T helper type 2 cell differentiation from precursor to effector activation. *Immunology*. 2013;140:31–38. doi:10.1111/imm.12121

35. Lipinski CA, Lombardo F, Dominy BW, et al. Experimental and computational approaches to estimate solubility and permeability in drug discovery and development settings. *Adv Drug Deliv Rev*. 2001;46:3–26. doi:10.1016/S0169-409X(00)00129-0
36. Lin GY, Yao HC, Zheng XN, et al. Virtual screening for effective components in commonly used anti-diabetic traditional Chinese medicines based on molecular docking technology. *Chin J Ex Trad Med Form*. 2015;21:202–206. doi:10.13422/j.cnki.syfjx.2015150202
37. Amano W, Nakajima S, Yamamoto Y, et al. JAK inhibitor JTE-052 regulates contact hypersensitivity by downmodulating T cell activation and differentiation. *J Dermatol Sci*. 2016;84:258–265. doi:10.1016/j.jdermsci.2016.09.007
38. Welsch K, Holstein J, Laurence A, et al. Targeting JAK/STAT signalling in inflammatory skin diseases with small molecule inhibitors. *Eur J Immunol*. 2017;47:1096–1107. doi:10.1002/eji.201646680
39. Yang JH, Yoo JM, Cho WK, et al. Anti-inflammatory effects of Sanguisorbae Radix water extract on the suppression of mast cell degranulation and STAT-1/Jak-2 activation in BMMCs and HaCaT keratinocytes. *BMC Complement Altern Med*. 2016;16:347. doi:10.1186/s12906-016-1317-4
40. Hazzalin CA, Mahadevan LC. MAPK-regulated transcription: a continuously variable gene switch ? *Nat Rev Mol Cell Biol*. 2002;3:30–40. doi:10.1038/nrm715
41. Wang ZG, Yi T, Long M, et al. Electro-acupuncture at Zusanli acupoint (ST36) suppresses inflammation in allergic contact dermatitis via triggering local IL-10 production and inhibiting p38 MAPK activation. *Inflammation*. 2017;40:1351–1364. doi:10.1007/s10753-017-0578-5
42. Wu XT, Qi XY, Wang J, et al. Paeoniflorin attenuates the allergic contact dermatitis response via inhibiting the IFN-γ production and the NF-κB/IκBα signaling pathway in T lymphocytes. *Int Immunopharmacol*. 2021;96:107687. doi:10.1016/j.intimp.2021.107687
43. Zhou Y, Yang QY, Xu H, et al. miRNA-221-3p enhances the secretion of Interleukin-4 in Mast cells through the phosphatase and tensin homolog/p38/nuclear factor-kappaB pathway. *PLoS One*. 2016;11:e0148821. doi:10.1371/journal.pone.0148821
44. Jegal J, Park NJ, Lee SY, et al. Quercitrin, the main compound in Wikstroemia indica, mitigates skin lesions in a mouse model of 2,4-Dinitrochlorobenzene-induced contact hypersensitivity. *Evid Based Complement Alternat Med*. 2020;2020:4307161. doi:10.1155/2020/4307161
45. Park SA, Bong SK, Lee JW, et al. Diosmetin and its glycoside, diosmin, improve Atopic Dermatitis like lesions in 2,4-Dinitrochlorobenzene-induced murine models. *Biomol Ther*. 2020;28:542–548. doi:10.4062/biomolther.2020.135
46. Lee DH, Park JK, Choi J, et al. Anti-inflammatory effects of natural flavonoid diosmetin in IL-4 and LPSinduced macrophage activation and atopic dermatitis model. *Int Immunopharmacol*. 2020;89:107046. doi:10.1016/j.intimp.2020.107046
47. Lim H, Park H, Kim HP. Inhibition of contact dermatitis in animal models and suppression of proinflammatory gene expression by topically applied flavonoid, wogonin. *Arch Pharm Res*. 2004;27:442–448. doi:10.1007/BF02980087
48. Lim H, Park H, Kim HP. Effects of flavonoids on matrix metalloproteinase-13 expression of Interleukin-1 beta-treated articular chondrocytes and their cellular mechanisms: inhibition of c-Fos/AP-1 and JAK/STAT signaling pathways. *J Pharmacol Sci*. 2011;116:221–231. doi:10.1254/jphs.11014fp
49. Rolfe HM. A review of nicotinamide: treatment of skin diseases and potential side effects. *J Cosmet Dermatol*. 2014;13(4):324–328. doi:10.1111/jocd.12119
50. Arakawa T, Sugiyama T, Matsuura H, et al. Effects of supplementary Seleno-L-methionine on Atopic Dermatitis-like skin lesions in mice. *Biol Pharm Bull*. 2018;41(9):1456–1462. doi:10.1248/bpb.b18-00349
51. Agus A, Planchais J, Sokol H. Gut microbiota regulation of tryptophan metabolism in health and disease. *Cell Host Microbe*. 2018;23(6):716–724. doi:10.1016/j.chom.2018.05.003
52. Fang ZF, Pan T, Li LZ, et al. Bifidobacterium longum mediated tryptophan metabolism to improve atopic dermatitis via the gut-skin axis. *Gut Microbes*. 2022;14(1):2044723. doi:10.1080/19490976.2022.2044723